**Ocean Science
Discussions**

Eastern Mediterranean biogeochemical flux model: simulations of the pelagic ecosystem

G. Petihakis[1], G. Triantafyllou[1], G. Korres[1], A. Pollani[1], and I. Hoteit[2]

[1]Institute of Oceanography, Hellenic Center for Marine Research, P.O. BOX 2214,
Iraklion-Crete, GR 71003, Greece
[2]Scripps Institution of Oceanography, La Jolla, CA, USA

Correspondence to: G. Petihakis (pet@her.hcmr.gr)

OSD

3, 1349–1398, 2006

**Eastern
Mediterranean
biogeochemical flux
model**

G. Petihakis et al.

Title Page

Abstract	Introduction
Conclusions	References
Tables	Figures

◄◄	►►
◄	►
Back	Close

Full Screen / Esc

Printer-friendly Version

Interactive Discussion

EGU

Abstract

During the second phase (2003–2006) of the Mediterranean ocean Forecasting System Project (MFS) named Toward Environmental Predictions (MFSTEP) one of the three major aims was the development of numerical forecasting systems. In this context a generic Biochemical Flux Model (BFM) was developed and coupled with hydrodynamic models already operating at basin scale as well as at regional areas. In the Eastern Mediterranean basin the BFM was coupled with the Aegean Levantine Eddy Resolving MOdel (ALERMO). The BFM is a generic highly complex model based on ERSEM and although a detailed description of the model and its sub models is beyond the scope of this work a short presentation of the main processes, paying emphasis on the parameter values used is presented. Additionally the performance of the model is evaluated with some preliminary results being qualitatively compared against field observations. The model at its present form is rather promising reproducing all major important features even though there are inefficiencies mostly related to primary and bacterial productivity rates.

1 Introduction

The Mediterranean basin displays a great variety of climatic, physical, ecological, social, economic and cultural traits. Nevertheless and in spite of the apparent diversity the Mediterranean region has long been recognised as a single functional climatic, ecological, economic and social system. Thi semi-enclosed sea, which represents only 0.69% of the global ocean surface and 0.27% of the global ocean volume, contains several deep basins and a number of large, relatively shallow bays. The length of the Mediterranean coastline is about 45 000 km, 18 000 km of which is the coastline of Mediterranean islands. Some of the largest rivers of Europe and Africa drain their nutrients and sediment rich waters into the Mediterranean. About 92% of the estimated natural riverine input of 15 000 m^3/s is from the northern shores. However the manage-

1350

ment of these inputs has significantly reduced their discharge influencing large areas of the basin. In order to balance the approximately 3250 km^3/yr water loss (Evaporation – Precipitation – Rivers – Black Sea) there is an influx of Atlantic waters through the straits of Gibraltar. Considering that the present population in the coastal areas around the basin is estimated at over 120 millions and another 100–50 million tourists visit those areas annually, it becomes easy to understand the importance of this sea and the need for management practices.

From the early studies on the Mediterranean system (McGill, 1965; Mihailov, 1964) it became evident that the basin is characterised as oligotrophic, while later ones (Moutin and Raimbault, 2002) demonstrated a well defined eastward decreasing trend in primary productivity. Although initially this was attributed to the small river discharges and the absence of major upwelling areas (Azov, 1991), the main responsible mechanism is the anti-estuarine circulation. Thus surface Atlantic Water (AW) low in salinity and nutrients enters the basin at Gibraltar and after following the north coast of Africa reaches the central Levantine basin. There at selected areas during winter cooling, it increases in density and sinks at ∼300 m forming the Levantine Intermediate Water (LIW), a water mass saltier and rich in dissolved nutrients (Theocharis et al., 1993). LIW following a parallel course with AW but with an opposite direction, eventually outflows into the Atlantic (Pinardi and Masetti, 2000) contributing to the impoverishment of the basin.

There are two distinct basins in the Mediterranean separated by the shallow Sicily Strait (∼500 m) which limits exchange, decoupling thus hydrodynamic and ecological conditions (Crise et al., 1999). The Eastern Mediterranean is an unusual and unique marine ecosystem as despite receiving considerable inputs of natural and anthropogenic nutrients it is ultra-oligotrophic (Krom et al., 2003). The anti-estuarine circulation in the eastern basin due to the higher evaporation over precipitation in conjunction with the very low terrestrial inputs since Aswan dam in 1965, has created one of the most oligotrophic areas of the world (Azov, 1991). The concentrations of dissolved nutrients in the deep waters are much lower than those in other oceans and

when mixed into the surface layers they support very low primary productivity, with a deep chlorophyll maximum (DCM) deeper than 100 m. Some other characteristics are a high content of pico- and nano-plankton in the offshore regions while microplankton and eukaryotes only become important in coastal regions and upwelling areas (Krom et al., 2003). As in other oligotrophic systems an important biological component in this basin is the heterotrophic bacteria which in the euphotic zone their carbon biomass is of the same order of magnitude as that of phytoplankton (Zohary and Robarts, 1998). The circulation of the Eastern Mediterranean is complex with a number of basin-scale, sub-basin-scale and mesoscale structures where permanent recurrent and transient cyclonic and anticyclonic eddies are interconnected by jets and currents, although both structures and mechanisms are under debate (Alhammoud et al., 2005). Among the most persistent mesoscale features are the Rhodes gyre a cold-core eddy southwest of Rhodes, the Cyprus eddy a warm-core eddy south of Cyprus and the Mersah Matru eddy southeast of Crete (Theocharis et al., 2002). The complex morphological structure of the eastern basin and its exchanges with the western basin make the circulation particularly unsteady and variable with changes in the thermohaline circulation strongly interacting with the productivity of surface waters.

During the second phase (2003–2006) of the Mediterranean ocean Forecasting System Project (MFS) named Toward Environmental Predictions (MFSTEP) there were three major aims a) the Near Real Time Observing system; b) the numerical forecasting systems at basin scale and for regional areas; c) the forecast products dissemination/exploitation system. One of the six major scientific/technological objectives was the "implementation of three dimensional ecosystem models coupled to the forecasting system for future predictions of biochemical fluxes and state variables". The last few years the computing resources and numerical modelling systems have become mature enough to use them to address the ambitious task of reproducing, explaining and predicting the evolution of marine ecosystems and their response to the variability of physical forcing. Thus a generic Biochemical Flux Model (BFM) based on ERSEM III (Vichi et al., 2004) was developed and coupled with existing hydrodynamic models de-

veloped during the Mediterranean ocean Forecasting System Pilot Project (MFSPP). Considering that primary production processes particularly in oligotrophic systems are strongly linked to the variability in physical forcing, a correct representation of the current structures is an undisputable requirement if one wants to achieve any trustworthy
⁵ representation for the lower trophic levels. The accurate simulation of the spatial and temporal variability of the physical and biogeochemical characteristics of the Mediterranean marine ecosystem is a fully coupled coastal-open ocean problem requiring the solution of a fully three-dimensional density driven general circulation problem, together with the appropriate description of ecological and biogeochemical processes. The
¹⁰ modelling of marine ecosystems is lagging behind the modelling of marine physics, as in contrast to the simulation of the atmosphere or ocean where a basic description of the physics is provided by the Navier-Stokes equations of fluid dynamics (Gill, 1982) there is no basic set of equations that describe the ocean ecosystem. Additionally it requires robust hydrodynamic models and adequate computing resources. However in
¹⁵ the past 10 years significant progress has been made with a number of different hydrodynamic and biogeochemical numerical models being developed and implemented in the Mediterranean with varying degrees of complexity, and resolution.

In this work the coupling of the BFM with the Aegean Levantine Eddy Resolving MOdel (ALERMO) (Korres and Lascaratos, 2003) in the Eastern Mediterranean is de-
²⁰ scribed together with the application, calibration and preliminary validation of the coupled models.

2 Model

2.1 Model description

The ALERMO model (Korres and Lascaratos, 2003) is based on the Princeton Ocean
²⁵ Model (POM) (Blumberg and Mellor, 1978; Blumberg and Mellor, 1987), extensively described in literature and accompanied by a comprehensive user's guide (Mellor, 1998).

Title Page

Abstract | Introduction

Conclusions | References

Tables | Figures

◄◄ | ►►

◄ | ►

Back | Close

Full Screen / Esc

Printer-friendly Version

Interactive Discussion

Eastern Mediterranean biogeochemical flux model

G. Petihakis et al.

It is a primitive equation, 3-D model, with a bottom following vertical sigma coordinate system, a free surface and a split mode time step while temperature, salinity, velocity and surface elevation are prognostic variables.

An important factor in the system of the Eastern Mediterranean is the inflow of brackish and fresh waters from the Dardanelles and the various major riverine systems respectively. In particular the approximately 300 km^3/y brackish waters entering the Aegean from the Dardanelles are considered to strongly affect the dynamics of North and Central Aegean (Lykousis et al., 2002). Additionally the contribution of the main Greek rivers (Evros, Aliakmonas, Nestos and Axios) although much smaller compared to the Dardanelles outflow ($\sim$19 km^3/y), are considered to significantly contribute towards a more productive system in the North Aegean. Finally a biologically significant riverine system is the Nile at the north coast of Africa with an approximately 63 km^3/y influx of fresh waters.

ALERMO includes parameterisation of both Dardanelles and major riverine systems. The net inflow into the Aegean from Dardanelles is approximated to 10^4 m^3/s with a seasonal modulation of 5×10^3 m^3/s. Maximum values are reached during mid-July and minimum values during mid-January with a constant salinity of 28.3 psu. The three Greek rivers are set according to daily climatological values provided by the Greek Ministry of Agriculture, ranging from 28 to 324 m^3/s, with maximum values during February and minimum values during July. As already mentioned the salinity at Dardanelles is set to 28.3 psu while for the rivers to 0. The temperature of the inflows is set at the same values with the model's top layer at the specified grid point. Although this parameterisation might produce an underestimation compared to a lateral flux boundary condition, the absence of detailed data on inflow and outflow velocities at the straits renders it a more accurate approach.

The coupling between the physics and the biology is done through advection-diffusion equations:

$$\frac{\vartheta C}{\vartheta t} = -U\frac{\partial C}{\partial x} - V\frac{\partial C}{\partial y} - W\frac{\partial C}{\partial z} + \frac{\partial}{\partial x}\left(A_H\frac{\partial C}{\partial x}\right) + \frac{\partial}{\partial y}\left(A_H\frac{\partial C}{\partial y}\right) + \frac{\partial}{\partial z}\left(K_H\frac{\partial C}{\partial z}\right) + \sum BF \quad (1)$$

**Eastern
Mediterranean
biogeochemical flux
model**

G. Petihakis et al.

where U, V, W the velocity field components, A_H the horizontal viscosity coefficient, and K_H the vertical eddy mixing coefficient, provided by POM. The last term accounts for the total biochemical flux, for each pelagic group. Along the open boundary the ecosystem pelagic state variables are described by solving water column 1-D ecosys-
tem models at each surface grid point on the open boundary. The ecological model accounts for the nutrients inputs from the north Greece rivers, the Dardanelles and the Nile river. The annual nutrients concentrations in terms of phosphate, nitrate and ammonium in the north Greece rivers are set to 3.8, 30.64 and 2.8 mmol/m^3 for Evros, 3.2, 31.93 and 6.38 mmol/m^3 for Axios and Aliakmonas and 4.0, 20.0 and 3.95 mmol/m^{3}for
Nestos. Nutrient concentrations for the Nile delta are set to 10.52 and 32.25 mmol/m^3 for phosphate and nitrate respectively. Finally the Dardanelles inflowing waters to the north Aegean sea are assumed to have nutrients concentrations of 0.09, 0.33 and 0.15 mmol/m^3 in terms of phosphate, nitrate and ammonium respectively, while POM and DOM concentrations are set to 10.0,1.0 and 0.1 mgrC/m^3 (C, N, P) and 8.0, 0.65
and 0.07 mgrC/m^3 (C,N,P),

   The BFM is a continuation of the generic highly complex model ERSEM (Baretta et al., 1995) and in particular in its last version ERSEM III (Vichi et al., 2004). Although a detailed description of the BFM and its sub models is beyond the scope of this paper a short presentation of the code, as well as the parameter values used in the Eastern
Mediterranean, is given further in the paper. This is considered necessary as its modular structure in conjunction with the open source allows the inclusion or modification of the processes from the standard version. Additionally it will be helpful for those not familiar with the model or for those interested on the particular parameterisation. As many times described, the model includes physical, chemical and biological processes
which display a coherent system behaviour. Unlike those models using a classification based on genera or species assemblages, it uses a functional group approach – no phylogenetic meaning – where each group is composed of many different species with common biogeochemical and /or ecological functions, separating the organisms according to their trophic level (producers, consumers and decomposers) and further

G. Petihakis et al.

subdivided on the basis of their trophic links and/or size (Fig. 1). Although within each trophic level the groups have the same processes, differentiation is achieved through the different parameter values. All the important physiological (ingestion, respiration, excretion and egestion), and population (growth, migration and mortality) processes are included, and are described by fluxes of carbon and nutrients. Carbon is the basic unit cycled in the system, followed by macronutrients and oxygen, with each state variable having up to five vector components (C, N, P, Si, Chl-a), with variable carbon/nutrients and carbon/chl-a ratios.

The model state variables, together with the respective constituents and the notation used are given in Table 1. According to the food web matrix as modulated for the Eastern Mediterranean (Table 2) diatoms (P1) are preyed by omnivorous mesozooplankton (Z4), nano-phytoplankton (P2) by heterotrophic nanoflagellates (Z6) and mostly by microzooplankton, pico-phytoplankton (P3) mostly by heterotrophic nanofalgellates and to a lesser extent by microzooplankton and finally large phytoplankton (P4) by omnivorous mesozooplankton. Bacteria (B1) consume DOC both labile and semi-labile (R1 & R2), act as decomposers on POC (R6) and compete with phytoplankton for inorganic nutrients. Their main predators are the heterotrophic nanoflagellates while a small part is also channelled to microzooplankton. Heterotrophic nanoflagellates are preyed by microzooplankton which in turn is eaten by omnivorous mesozooplankton. Omnivorous mesozooplankton is preyed by carnivorous mesozooplankton (Z3) which is the top predator at the food chain, while in all consumers (Z6, Z5, Z4, Z3) there is feeding within the same functional group (cannibalism), acting as a stabilizing mechanism.

2.1.1 Primary producers

Phytoplankton comprise four groups; with P1 and P4 representing cells with the same Equivalent Spherical Diameter (ESD) of 20–200 μ, but with the former exhibiting an affinity for silica as diatoms do in natural conditions. P2 have an ESD of 2–20 μ and P3 of 0.2–2 μ representing nanophytoplankton and picophytoplankton respectively. All parameter values of this group are given in Tables 3 and 4. The rate of change for each

group can be described by the following text equation:

$$\frac{dP}{dt} = \text{photosynthesis} - \text{respiration} - \text{excretion} - \text{grazing} \tag{2}$$

Gross photosynthetic production is modulated by maximum productivity rate (p_sum), temperature response (et), light limitation (eiPI), and present biomass (PIc). In case of P1 the external silicate concentration is also taken into account in a form of a limitation factor (eN5s).

$$\text{photosynthesis} = \text{p\_sum} * \text{et} * \text{eN5s} * \text{eiPI} * \text{PIc} \tag{3}$$

Although P1 and P4 are considered as having the same size the latter have a lower maximum productivity rate as shown in Table 4. The temperature response is the same for all groups and has an exponential form.

$$et = e^{\left(\log(\text{p\_q10}) * \frac{\text{ETW} - \text{BASETEMP}}{\text{BASETEMP}}\right)} \tag{4}$$

where p_q10 is the characteristic temperature coefficient of each group indicating a doubling of reaction rate with a 10°C increase of the ambient temperature (ETW) relative to the reference temperature (BASETEMP). The choice of the reference temperature value is a challenging issue as the value used in the North Sea (10°C) is well below the reference temperature of the productive layer of the Eastern Mediterranean. The BFM formulation has a smaller gradient with respect to ERSEM III as shown in Fig. 2, which is further decreased with higher reference values.

Light limitation is computed according to the relation:

$$\text{eiPI} = 1 - e^{\left(-\frac{\text{qchlPc} * \text{p\_alpha\_chl}}{\text{p\_sum} * \text{et} * \text{eN5s} * \text{Irr}}\right)} \tag{5}$$

where qchlPc is the Chl:C ratio, p_alpha_chl the initial slope of the P-I curve, and Irr the photosynthetic irradiance parameterised according to Lambert-Beer formulation with extinction coefficients (in addition to the background) for suspended particles, silt, and phytoplankton shelf shading.

Title Page

Abstract | Introduction

Conclusions | References

Tables | Figures

◄◄ | ►►

◄ | ►

Back | Close

Full Screen / Esc

Printer-friendly Version

Interactive Discussion

EGU

Silicate limitation is a function of the external dissolved silicate concentration N5s where *p_chPs* is the half saturation constant of silicate in the water.

$$eN5s = \frac{N5s}{N5s + p\_chPs} \tag{6}$$

Respiration has two parts, the basal which is independent of growth modulated by the biomass, the temperature response (et) and the specific constant respiration rate (p_srs), and the activity respiration. The latter is a constant fraction (p_pu_ra) of the assimilated carbon i.e. photosynthesis – excretions. It is due to the basal respiration that under low light conditions the net primary production can become negative.

$$respiration = \left(\overbrace{et * p\_srs * Plc}^{BASAL} \right) + \left(\overbrace{p\_pu\_ra * (photosynthesis - excretions)}^{ACTIVITY} \right) \tag{7}$$

The processes of nutrient stress lysis of ERSEM III has been replaced with the excretion of dissolved carbohydrates. As seen so far, gross photosynthetic production is not dependent on the external nutrient supply (with the exception of silica for diatoms), which means that the cell can produce carbon even at very low nutrient concentrations. Thus a fixed proportion of the carbon (p_pu_ea) produced is channelled to dissolved carbohydrates (R2)

$$excretion = photosynthesis * p\_pu\_ea \tag{8}$$

while the rest can be assimilated or excreted according to the actual nutrient uptake and the minimum internal nutrient/carbon ratio (p_qnlc, p_qplc).

The grazing term refers to zooplankton predation analysed further in the manuscript with the flux to each predator mainly controlled by the food matrix increasing thus the generic nature of the model.

Nutrient uptake (uptake$_{total}$) is constrained between the maximum possible uptake for the present biomass (uptake$_{max}$) and the required uptake which is the sum of the

uptake due to net production (uptake$_{netprod}$) and the uptake necessary to cover internal shortages (uptake$_{miss}$).

$$\text{uptake}_{total} = \min\left(\text{uptake}_{max}, \left(\text{uptake}_{netprod} + \text{uptake}_{miss}\right)\right) \tag{9}$$

The maximum possible uptake (uptake$_{max}$) is a function of external nutrient concentration, the present biomass (PIc) and the uptake parameter (p_qun) for the particular nutrient (Aksnes and Egge, 1991) and is a measure for the cell for the trophic status of the surrounding water. In case of nitrogen there is also a partition between nitrate (N3n) and ammonium (N4n).

$$\text{uptake}_{max} = \left(\overbrace{\text{p\_qun} * \text{N3n} * \text{PIc} * \left(\frac{\text{p\_lN4}}{\text{p\_lN4} + \text{N4n}} \right)}^{\text{uptake}_{max\_N3n}} \right) + \left(\overbrace{\text{p\_qun} * \text{N4n} * \text{PIc}}^{\text{uptake}_{max\_N4n}} \right) \tag{10}$$

The half saturation value (p_lN4) controls the nitrate uptake with small cells (p_lN4 = 0.1) having a preference for ammonium as shown in Fig. 3.

The uptake due to net production (uptake$_{netprod}$) is regulated by the productivity (photosynthesis – respiration – excretion).

$$\text{uptake}_{netprod} = \text{productivity} * \text{p\_xqn} * \text{p\_qnRc} \tag{11}$$

where p_qnRc the Redfield N/C ratio and p_xqn the multiplication factor accounting for higher uptake compared to carbon (luxury uptake).

The missing nutrient uptake (uptake$_{miss}$) is a function of the maximum internal Nutrient/Carbon ratio having subtracted the structural part (PIn) multiplied with the net growth rate, a representation of an adaptation mechanism to the current conditions (sadap).

$$\text{uptake}_{miss} = (\text{p\_xqn} * \text{p\_qnRc} * \text{PIc} - \text{PIn}) * \text{sadap} \tag{12}$$

Title Page

Abstract | Introduction

Conclusions | References

Tables | Figures

|◄ | ►|

◄ | ►

Back | Close

Full Screen / Esc

Printer-friendly Version

Interactive Discussion

EGU

If the uptake is +ve then the nitrogen flow into the cell is partitioned between nitrate and ammonium

$$uptake_{N3n} = \frac{uptake_{total} * uptake_{max\_N3n}}{uptake_{max}}$$

$$uptake_{N4n} = \frac{uptake_{total} * uptake_{max\_N4n}}{uptake_{max}} \tag{13}$$

5   while in the case that the internal nitrogen has exceeded the maximum internal ratio the uptake becomes –ve and the surplus is excreted in the form of ammonium.

The same processes are used for phosphorus and silicate but in the latter there is no internal storage and thus uptake is dependent on the appropriate Redfield ratio (p_qsRc).

10   In the early versions of ERSEM (I & II) chlorophyll was a diagnostic variable calculated from the cell carbon content with an assumed constant ratio. Although this simplification at the first steps of the model could be justified, the significant variability of C/Chl ratio (23–79) (Parsons et al., 1973) forced for an upgrade in ERSEM III with the introduction of chlorophyll as a state variable (*Phytoi*) (Vichi et al., 2004). Subsequently

15   in BFM the synthesis is controlled by the productivity (photosynthesis – respiration – excretion), the maximum Chl/C ratio (rho_Chl) and the intracellular nitrogen limitation factor (iNIn), while there is also a turnover/destruction term.

$$rate\_chl = iNIn * rho\_Chl * productivity - destruction \tag{14}$$

The maximum Chl/C ratio is calculated as:

20   $$rho\_Chl = \frac{p\_qchlc * photosynthesis * PIc}{p\_alpha\_chl * (phytoi + 1) * Irr} \tag{15}$$

where (p_qchlc) the maximum Chl/C ratio for each group. The intracellular nitrogen limitation factor is constrained between the range 0–1 and follows Droop kinetics (Droop,

Eastern Mediterranean biogeochemical flux model

G. Petihakis et al.

Title Page

Abstract   Introduction

Conclusions   References

Tables   Figures

◄   ►►

◄   ►

Back   Close

Full Screen / Esc

Printer-friendly Version

Interactive Discussion

EGU

1974). It is a function of the actual internal cell N/C ratio (qnPc) and the Redfield ratio (p_qnRc) having subtracted the structural content of the cell (minimum N/C ratio) (p_qnlc).

$$\text{iNIn} = \min\left(1.0, \max\left(0.0, \frac{\text{qnPc} - \text{p\_qnlc}}{\text{p\_qnRc} - \text{p\_qnlc}}\right)\right) \tag{16}$$

5 Intracellular limitation factors are calculated accordingly for phosphorus and silicate while in this particular application for the total limitation factor the Liebig rule is used (min).

Finally sedimentation of phytoplankton is the product of a background sinking parameter (p_rPim) and the sinking due to nutrient limited conditions according to a threshold
10 value (p_esNI), the total nutrient limitation factor (tN), and the sedimentation rate parameter (p_res). In this way the phytoplankton can move from a nutrient limited area to an area where there are nutrients, a significant process in patchy systems such as the Eastern Mediterranean basin.

$$\text{sedimentation} = \overbrace{\text{p\_rPim}}^{\text{Background}} + \overbrace{\text{p\_res} * \max\left(0.0, (\text{p\_esNI} - \text{tN})\right)}^{\text{NutrientLimitation}} \tag{17}$$

15 The total nutrient limitation factor (tN) is calculated by the intracellular nitrogen (INin) and phosphorus (IN1p) (also silicate for diatoms) limitation factors with a triple user choice. Thus the first is the root of the multiplied limitations, the second takes the most limiting nutrient (used in this application) and the third considers a ratio of the two.

2.1.2 Decomposers

20 Although from the beginning of ERSEM there was only bacteria filling the role of decomposers (Baretta-Bekker et al., 1995), significant changes have been introduced in following versions (Allen et al., 2004; Baretta-Bekker et al., 1997; Blackford et al., 2004a; Vichi et al., 2004). BFM pelagic bacteria (B1) (Table 5) are a wide group comprising free living heterotrophic bacteria utilizing dissolved (R1) and particulate (R6)
25 detritus under both aerobic and anaerobic processes.

Eastern Mediterranean biogeochemical flux model

G. Petihakis et al.

The bacterial rate of change is described by the following text equation,

$$\frac{dB}{dt} = \text{uptake} - \text{respiration} - \text{mortality} - \text{predation} \tag{18}$$

Actual uptake is constrained between the potential uptake (uptake_{pot}) and the total available substrate (uptake_{sub})

$$\text{uptake} = \min\left(\text{uptake}_{pot}, \text{uptake}_{sub}\right) \tag{19}$$

Potential uptake represents the intrinsic potential for growth under the present environmental conditions and is a function of maximum productivity rate (p_sum), temperature response (et), intracellular nutrient limitation (iN), and present biomass (B1c).

$$\text{uptake}_{pot} = \text{p\_sum} * \text{iN} * \text{et} * \text{B1c} \tag{20}$$

nutrient limitation is constrained between the range 0–1 and unlike phytoplankton is a function of the actual internal cell N/C ratio (qnB1c) and the Redfield ratio (p_qnc), (in this case for nitrogen) without considering the structural component.

$$\text{iNIn} = \min\left(1.0, \max\left(0.0, \frac{\text{qnB1c}}{\text{p\_qnc}}\right)\right) \tag{21}$$

The total limitation (iN) follows also the Liebig rule among nitrogen and phosphorus.

The uptake due to substrate represents the available food and is partitioned among the different food sources. Both available labile DOM (R1) and carbohydrates (R2) are taken up according to the preference factors p_suR1 and p_suR2 respectively, while for the particulate component of detritus (R6) apart from the preference (*p_suR6*), the quality is also taken into consideration (suR6).

$$\text{uptake}_{sub} = \text{R1c} * \text{p\_suR1} + \text{R2c} * \text{p\_suR2} + \text{R6c} * \text{p\_suR6} * \text{suR6} \tag{22}$$

where suR6 is a factor of the most limited nutrient inside the available detritus, and is a function of the internal N/C and P/C ratios and the Redfield ratio for bacteria.

$$\text{suR6} = \min\left(\min\left(1.0, \frac{\text{qnR6c}}{\text{p\_qnc}}\right), \min\left(1.0, \frac{\text{qpR6c}}{\text{p\_qpc}}\right)\right) \tag{23}$$

Title Page

Abstract | Introduction

Conclusions | References

Tables | Figures

◄ | ►

◄ | ►

Back | Close

Full Screen / Esc

Printer-friendly Version

Interactive Discussion

EGU

Respiration is partitioned between basal which is formulated as in phytoplankton and activity respiration where a variable component has been introduced in order to differentiate between oxic and anoxic conditions.

$$\text{respiration} = \left(\overbrace{\text{et} * \text{p\_srs} * \text{B1c}}^{\text{BASAL}} \right) + \left(\overbrace{(1.0 - \text{p\_pu} + \text{p\_puo} * (1.0 - \text{eO2})) * \text{uptake}}^{\text{ACTIVITY}} \right) \quad (24)$$

where p_pu the assimilation efficiency under oxic conditions and p_puo the decrease in assimilation efficiency under anoxic conditions. The oxygen factor is a cubic Michaelis – Menten relation, of the available oxygen (O2o) and the oxygen concentration at which metabolic functionalities are halved (p_chdo).

$$\text{eO2} = \frac{\text{O2o}^3}{\text{O2o}^3 + \text{p\_chdo}^3} \quad (25)$$

This is a steep sigmoid curve giving an activity respiration value between 0.6 and 0.8 of the uptake (Fig. 4).

To partly account for viral lysis a mortality term is used with a constant mortality rate (p_sd) modulated by the temperature factor (et). Mortality is directed to the dissolved organic fraction (R1) for both carbon and nutrients.

$$\text{mortality} = \text{p\_sd} * \text{et} * \text{B1c} \quad (26)$$

A future improvement of the code will be the insertion of a density dependent mortality, which will account for the observed maximum bacterial biomass in the open ocean.

A much better but more complex approach will be the addition of viral module since viruses are the most common biological agents in the sea (Fuhrman, 1999; Heldal and Bratbak, 1991; Proctor and Fuhrman, 1990; Suttle et al., 1990). Viruses can affect a large number of organisms influencing many biogeochemical and ecological processes including nutrient cycling, system respiration, particle size distribution and sinking rates, bacterial and algal biodiversity and species distributions, algal bloom

EGU

control and genetic transfer (Bratbak et al., 1992; Fuhrman, 1999). The importance of this mechanism has been illustrated through experimental simulations with ERSEM having incorporated a viral module. Results indicated that when the bacteria were not limited by the availability of dissolved organic carbon, the virus acted to reduce bacterial production and enhance primary production. The ratio of primary to bacterial production changed from 4.83 without the virus to 8.27 with the virus indicating a shift away from a microbial loop dominated ecosystem. Conversely when bacteria were dissolved organic carbon limited, the virus acted to increase the turnover of dissolved organic carbon and to enhance bacterial production, which drove the system towards an increase in primary production as enhanced dissolved nutrient cycling enhanced dissolved inorganic nutrient availability. Although the turnover of carbon was enhanced there was no change in the trophic status as indicated by the ratio of primary to bacterial production which had a value of 2.15 in both cases.

Coming back to the BFM predation on bacteria is exerted mainly by heterotrophic flagellates (Z6) and to a small degree by microzooplankton (Z5). Bacteria can act as remineralisers excreting nutrients or as competitors to phytoplankton taking up nutrients depending on their internal Nutrient/Carbon ratios. Thus if the Nutrient/Carbon ratio of the food (dissolved and particulate) exceeds the Redfield ratio (p_qnc or p_qpc) then there is excretion to ammonium (N4n) or to phosphate (N1p) according to the present biomass and the net productivity rate.

$$\text{excretion} = \text{productivity}_{\text{rate}} * \left(\frac{\text{ruR6n} + \text{ruR1n}}{\text{uptake}} - \text{p\_qnc} \right) * \text{B1c} \tag{27}$$

In the case that the food is of low quality then there is uptake of inorganic nutrients.

Nutrient uptake (in this case for N) is separated into maximum uptake which considers filling an empty cell (B1c) according to the characteristic uptake parameter (p_qun) and the external nutrient concentration (N3n) with the same differentiation as in phyto-

plankton between nitrate and ammonium.

$$\text{uptake}_\text{max} = \left(\overbrace{\text{p\_qun} * \text{N3n} * \text{B1c} * \left(\frac{\text{p\_lN4}}{\text{p\_lN4} + \text{N4n}} \right)}^{\text{uptake}_{\text{max\_N3n}}} \right) + \left(\overbrace{\text{p\_qun} * \text{N4n} * \text{B1c}}^{\text{uptake}_{\text{max\_N4n}}} \right) \qquad (28)$$

2.1.3 Consumers

Consumers are represented by two major groups, the microzooplankton composed by
heterotrophic nanoflagellates and microzooplankton, and the mesozooplankton which
is divided into omnivorous and carnivorous mesozooplankton. The text equation describing the rate of change is:

$$\frac{dZ}{dt} = \text{uptake} - \text{respiration} - \text{mortality} - \text{excretion} - \text{predation} \qquad (29)$$

Uptake is a function of maximum growth rate (p_sum), temperature response (et), the
available food (efood) and the standing stock (Zlc).

$$\text{uptake} = \text{p\_sum} * \text{et} * \text{efood} * \text{Zlc} \qquad (30)$$

For the available food a Michaelis – Menten relation is used, considering the total
available food sources (rumc) – calculated by the available stocks and the food matrix
preference factor including a lower threshold parameter (p_minfood) in order to avoid
overexploitation – and the half saturation parameter (p_chuc) where food uptake is 0.5
of maximum.

$$\text{efood} = \frac{\text{rumc}}{\text{rumc} + \text{p\_chuc}} \qquad (31)$$

In the case of mesozooplankton the Michaelis – Menten relation is modulated by a
search volume parameter (p_vum), the total available food (Zlm) and the maximum

growth rate (p_sum) while there is no lower threshold parameter constraining ZIm.

$$\text{efood} = \frac{\text{p\_vum} * \text{Zim}}{\text{p\_vum} * \text{Zim} + \text{p\_sum}} \qquad (32)$$

Once the actual uptake is estimated the contribution of each food source is calculated according to the ratio of uptake/total available food (rumc or ZIm).

Respiration has two components, the temperature dependent basal respiration and the activity respiration.

$$\text{respiration} = \left(\overbrace{\text{et} * \text{p\_srs} * \text{Zlc}}^{\text{BASAL}} \right) + \left(\overbrace{((1.0-\text{p\_pu}) * (1.0-\text{p\_pu\_ea})) * \text{uptake}}^{\text{ACTIVITY}} \right) \qquad (33)$$

where p-srs the characteristic rest respiration rate of the particular functional group, p_pu the assimilation efficiency and p_pu_ea the excreted fraction of uptake.

Mortality is handled differently between microzooplankton and mesozooplankton with the former group being coupled to the oxygen regime. Thus the constant background mortality rate (p_sd) is increased according to the oxygen conditions, modulated by a low oxygen mortality rate (p_sdo) and an oxygen limitation factor (eO2) calculated from the relative oxygen saturation and a half saturation parameter.

$$\text{mortality} = ((1.0-\text{eO2}) * \text{p\_sdo} + \text{p\_sd}) * \text{Zlc} \qquad (34)$$

Mesozooplankton mortality is composed by the natural mortality affected by temperature and the density dependent mortality modulated by a constant low oxygen mortality rate (p_sdo) and a density dependent mortality (p_sds) term.

$$\text{mortality} = \left(\overbrace{\text{p\_sd} * \text{et} * \text{Zlc}}^{\text{NATURAL}} \right) + \left(\overbrace{\text{p\_sdo} * \text{Zlc}^{\text{p\_sds}}}^{\text{DENSITY DEPENDENT}} \right) \qquad (35)$$

Eastern Mediterranean biogeochemical flux model

G. Petihakis et al.

Title Page

Abstract · Introduction

Conclusions · References

Tables · Figures

◄ · ►|

◄ · ►

Back · Close

Full Screen / Esc

Printer-friendly Version

Interactive Discussion

EGU

Excretion is a function of the assimilation efficiency (p_pu) of each group and the excreted fraction of uptake (p_pu_ea).

$$\text{excretion} = \text{uptake} * (1.0 - \text{p\_pu}) * \text{p\_pu\_ea} \tag{36}$$

The mortality and excretion products in the case of microzooplankton are apportioned between dissolved and particulate detrital components according to a parameter (p_pe_R1) with a highest proportion towards DOM. For mesozooplankton excretion is a fraction of the total food uptake (p_peI_R6) while all products are directed to the particulate detrital pool.

Nutrient uptake is through feeding according to the nutrient to carbon ratio of each food prey. The same approach is used in the excretions with nutrient being coupled to carbon following the internal nutrient to carbon ratio. To avoid excess nutrients being built up inside the consumer pools, any amounts higher than the maximum allowed nutrient to carbon ratios (p_qn_mz) are excreted to the inorganic pool (phosphate and ammonium) according to a dumping coefficient (p_stemp).

Summarizing the above described processes, the dissolved organic matter (R1) is produced by all groups except mesozooplankton and is consumed by bacteria while the particulate fraction (R6) is produced by all groups except bacteria which are the only consumers. The semi-labile carbohydrates (R2) produced during phytoplankton limitation are exclusively used by bacteria. Water column processes such as nitrification, denitrification, reoxidation of reduction equivalents and regeneration of dissolved silica are all included in the model, and are functions of water temperature and the appropriate parameters (Table 5).

2.2 Model set-up

The ALERMO hydrodynamic model has a horizontal resolution of $1/10° \times 1/10°$, 24 sigma layers in the vertical and an open boundary at $20°$ E. In order to have a better representation of the biological processes near the surface and a realistic surface and bottom boundary layer, a logarithmic distribution in the vertical layers has been chosen

Title Page

Abstract | Introduction

Conclusions | References

Tables | Figures

◀ | ▶|

◀ | ▶

Back | Close

Full Screen / Esc

Printer-friendly Version

Interactive Discussion

EGU

near the surface and the bottom. The model bathymetry was constructed from the U.S. Navy Digital Bathymetric Data Base 5 ($1/12° \times 1/12°$) using linear interpolation for the mapping of the data onto the model's grid. At the open boundary climatological seasonal temperature and salinity profiles are prescribed in cases of inflow, while radiation conditions are used for the baroclinic and barotropic velocities normal to the boundary. As already mentioned the physicochemical and biological characteristics of the Eastern Mediterranean are highly dependent on the circulation patterns and in particular to the inflowing surface waters of Atlantic origin and outflowing of deeper Levantine Intermediate Waters which are satisfactorily described by such kind of open boundary conditions.

The model is forced with the monthly climatological wind stress, heat and freshwater flux fields derived from the 6-h ECMWF 1979–1993 re-analysis atmospheric data as described in Korres and Lascaratos (2003). These fields are mapped onto the model grid and are properly interpolated at every time step of model's integration. The interested reader is referred to Korres and Lascaratos (2003) for a detailed description of the derivation of this climatological data set. Additionally the precipitation data needed for the freshwater budget at the surface of the basin were taken from Jaeger (1976) monthly data set (horizontal resolution $5° \times 2.5°$).

3 Simulations

A significant problem often encountered in modelling works is the absence of adequate field data for the validation of the model. In particular the Eastern Mediterranean has been sporadically studied – with very fragmented data both in space and in time – not only compared to other parts of the EU but even to the Western Mediterranean where high frequency monitoring stations have been established long time ago, both in coastal and offshore areas as in the case of DYFAMED station.

Moreover, the significant variability in the circulation patterns of the Eastern Mediterranean (Georgopoulos et al., 2000; Theocharis et al., 1999) and the strong coupling

Eastern Mediterranean biogeochemical flux model

G. Petihakis et al.

Title Page

Abstract | Introduction

Conclusions | References

Tables | Figures

|◄ | ►|

◄ | ►

Back | Close

Full Screen / Esc

Printer-friendly Version

Interactive Discussion

with the biological processes (Tselepides and Polychronaki, 1996) has made it evident that sparse spatial and temporal observations are prone to misrepresentation of the underlying dynamics. Until now studies of biological processes in the Eastern Mediterranean Sea have been focused on various spatial scales (large to mesoscale) in numerous campaigns (POEM, PELAGOS, MATER, INTERREG-N.AEGEAN, METROMED, ANREC, KEYCOP); however these studies were at the best seasonal. Only two studies on the annual cycle of biological and chemical parameters were performed one in the Cretan Sea during CINCS project (Tselepides and Polychronaki, 1996) and another one in the Cilician Basin (Eker-Develi et al., 2006), with no data however on phytoplankton, microzooplankton and mesozooplankton composition and biomass. Therefore there is still no study of the annual cycle combining all compartments of the planktonic food web, organic and inorganic nutrients and hydrology, in offshore waters.

Although the advances in satellite remote sensing techniques during the last twenty years allowed a considerable progress in the knowledge of spatial and temporal variations in algal biomass in various regions of the world ocean (Bricaud et al., 2002), the oligotrophic character of the Eastern Mediterranean (case I waters) requires a regionally tuned empirical algorithms. Comparisons of different ocean colour sensors (Bricaud et al., 2002) and different algorithms (Sancak et al., 2005) have shown that there are large overestimations at low chlorophyll levels <0.15 mg/m^3 and although alternative algorithms have been proposed non of those has been widely accepted yet.

In the above problem one has to add the significant variety of analytical methods, the limited access on raw data and the absence of in-situ sensor calibration information particularly as both phosphate and nitrate in the upper euphotic zone are close to the limits of detections.

From the above becomes evident that the validation of an ecosystem model forced climatologically in the highly variable environment of the Eastern Mediterranean is an open question. To overcome part of this problem a 1D version of the model was applied in the data rich M3A station, north of Heraklion in Crete, as this particular station

has been an ERSEM validation location during Mediterranean Forecasting System Pilot Project (MFSPP). To asses the performance of a complex model to a large extent depends on the time spent tuning unconstrained parameters with a large number of degrees of freedom. The problem of such exercise is that the model may begin to fit noise in the observational data rather than the underlying functional relationships (Hood et al., 2006). It is thus significant that the model's performance is evaluated against a different data set than the one used for tuning. In this particular case the model was tuned with a data set acquired during CINCS project (Tselepides and Polychronaki, 1996) and is compared with a completely different data set during MFSPP. As shown in Fig. 5 the model follows quite closely the chl-a concentrations as measured by the buoy sensors with only exception the first half of the year in the deeper layer (115 m) where simulated concentrations are significantly lower. However as the 1-D setup is lacking a horizontal transport mechanism, such model behaviour is within the expected error. The other mismatch at the surface sensor during October can be possibly attributed to an extreme atmospheric event such as heavy dust deposition and to a lesser extent to a strong upwelling, enriching the surface layers with nutrients, as the signal although obvious at both 45m and 65m is considerably stronger in the top most layer.

Moving to the 3-D model, as the scope of this study is the presentation of the model structure and a preliminary validation, the model behaviour is compared against some general trends and qualitative characteristics of the system. Thus in Table 7 some key biological parameters measured in the North, South Aegean and west of Dardanelles during March and September (Ignatiades et al., 2002; Siokou-Frangou et al., 2002) are given.

Figure 6 shows the simulated average chl-a concentrations during the first 10 days of March and September. Model results show increased values in the coastal areas of the domain with Saronikos and Thermaikos exhibiting concentrations greater than 0.5 mg/m^3 as expected. Although the model values are in the correct measured range with a general decrease from March to September, this is not the case in the Cretan Sea where autumn concentrations as produced by the model are higher compared to

March and significantly higher compared to field measurements. Basin scale models have an intrinsic inefficiency at the coastal areas as the coastal systems strongly interact with the open ocean at the level of ecosystem functioning require thus a very high resolution to simulate transport and turbulence processes in the water column.

5 Higher simulated concentrations are also produced in the East Mediterranean basin compared to in-situ data with a characteristic coupling between the biology and the physics as shown by the spatial chl-a distribution. The phenomenon of patchiness is caused by mesoscale turbulence on scales of 1–100 km where ageostrophic motions cause strong local up- and down-welling, to which the plankton ecosystem responds

10 dramatically, giving modulation in plankton abundance and commensurate changes in primary and secondary production and in community structure. The existence of patchiness poses problems when one tries to obtain a statistically significant estimate of primary production from a limited number of samples collected by ship, or by remote sensing (ocean colour) and it also poses problems in designing large scale models of

15 the ecosystem, with grid-spacing too large to resolve mesoscale turbulence.

The effect of the inputs in the system and in particular Dardanelles, the riverine system in the north Greece and the Nile is shown in Fig. 7, where maximum integrated primary productivity rates are produced by the model. This trend is also evident in the field values even though there is significant variability both between March and

20 September as well as between the adjacent sampling stations within the same period. Thus according to the in-situ data in Table 7 the area in front of the Dardanelles is the most active in terms of primary productivity followed by the North Aegean, while in all three areas there is a higher rate in March compared to September. This general characteristic is exhibited by the model but at lower levels in regard of the maximum

25 attained concentrations values. It is interesting to note the differentiation between north and south parts of the model domain, with simulated productivity rates in the north coast of Africa and Israeli – Lebanese waters being higher during September.

As already mentioned one of the most prominent hydrological patterns of the Eastern Mediterranean is the existence of mesoscale eddies significantly affecting the biology

of the particular area. Such an eddy system is the Rhodes cold-core eddy the center of which is the site of the greatest phytoplankton productivity anywhere in the open Eastern Mediterranean, mainly by diatoms and other large cells while the Bacteria/Phyto ratio is significantly lower compared to the rest of the Levantine basin (Krom et al., 2003). Some of the characteristics of this eddy are the deep mixing down to 3000 m, the development of a Deep Chlorophyll Maximum (DCM) at approximately 60 m and the quite high nutrient concentrations during mixing. The model seems to reproduce this system as shown in the cross sections of Fig. 8, with waters being uplifted at the area of the eddy (28° E–30° E) during March and with a significant DCM being developed during September, although the core of this feature lies deeper at approximately 90 m. In the north – south cross sections on the same figure the model is more productive in respect to chl-a in the north parts during March but not in September where significant phytoplanktonic activity is taking place in the southern deeper parts of the basin following the nutricline.

Heterotrophic microbes are very important since a large proportion, up to or exceeding 50% of the total flux of matter and energy in marine food webs passes through such organisms by means of dissolved organic matter (Fuhrman, 1999). In oligotrophic waters the bacterial biomass; depth integrated over the euphotic zone often exceeds that of phytoplankton, although heterotrophic bacterial production is low, with population doubling times at a weekly rate. Even with this slow growth, bacteria consume amounts of organic carbon, which constitute a large fraction of primary production (Azam et al., 1983). Thus it is suggested that a relatively small phytoplankton biomass must turn over much faster than the bacteria in order to feed the larger bacterial biomass (Fuhrman, 1999). Protozoan grazing is generally assumed to be the major cause of bacterial mortality, although grazing rates may not always be sufficient to explain bacterial mortality (Heldal and Bratbak, 1991). From the field values of integrated bacterial production the only existing trend are the relatively increased values in the area around Dardanelles with North and South Aegean being at almost same levels and without a prominent differentiation between March and September. March model results are in

the right range with the inflow areas exhibiting increased bacterial production mainly due to dissolved organic inputs. In September the model is overestimating in the south Aegean producing a clear north to south gradient which is not however depicted in the bacterial biomass which is more uniformly distributed (not shown). Bacterial biomass simulations are more variable compared to the field measurements with values ranging from 400 mgC/m^2 in the north to 2000 mgC/m^2 in the south. It is interesting to note that the high bacterial production simulated in the south – east part of the domain in March is associated with a low bacterial biomass indicating an active top down control of bacteria. As with the chl-a the spatial variability of bacterial productivity illustrates the coupling between bacteria and hydrodynamics as due to their small size, bacteria can react very fast to the short changes of the extremely variable environment of the East Mediterranean. Due to their small size bacteria have a large surface to volume ratio and thus can uptake the limiting dissolved nutrients more efficiently compared to bigger organisms.

Picophytoplankton is a very important component of the food web in the Eastern Mediterranean as under such oligotrophic conditions, these cells have a competitive advantage over large phytoplankton cells such as diatoms, flagellates etc. Their small size allows them to grow and compete with the antagonistic bacteria over limiting nutrients. Thus picophytoplankton's contribution in the total biomass is very high ranging from 57% to 82% (Table 7). Although the simulations fail to reach the values measured around Dardanelles, model results (not shown) are satisfactory both in the north and south Aegean. As picophytoplankton another significant functional group, in this particular environment, is the heterotrophic nanoflagellates. These together with bacteria play a significant role in the development of a microbial loop, which is a rather dominant process for large parts of the area. The model follows the trend of the in-situ data with higher values in September and with an increasing gradient form north to south during the same month. It is characteristic that less oligotrophic parts such as the coastal areas, the area around Dardanelles as well as the two urban gulfs exhibit reduced levels compared with the outer parts of the basin.

4 Conclusions

At both national and European level there is a strong public demand for improved management of water quality in the seas. Politically this demand is expressed through legislation, regulations and European directives and through the creation of new environmental services and agencies, all of which provide a strong need for forecasting activities. Additionally there is a global commitment to climate prediction, which requires ocean forecasting. This has been expressed via a series of important international meetings, agreements and conventions relating to marine sciences, management of the sea, marine conservation and climate control. Modelling and forecasting the Mediterranean not only is required to sustain and manage a healthy coastal environment but is also of great benefit to the maritime industries, to the control of pollution, the management of fisheries, and the improvement of maritime conditions for tourists.

The major aim of the pilot project of the Mediterranean Forecasting System (MF-SPP) was the prediction of the marine ecosystem variability in the coastal areas up to the primary producers and from the time scales of days to months. Such a predictive capability was considered essential in order to sustain a healthy coastal environment and its management. It was acknowledged that such forecasting system would have two essential parts, an observing system and a numerical modelling/data assimilation component that can use the past observational information to optimally initialise the forecast. The above were based on the hypothesis that both hydrodynamics and ecosystem fluctuations in the coastal/shelf areas of the Mediterranean are intimately connected to the large scale general circulation. The follow up project MFSTEP (MFS – Towards Environmental Predictions) aimed for the further development of an operational forecasting system for the Mediterranean Sea. Due to the previously mentioned gap between physical and ecological models, during MFSPP only one-dimensional ecosystem models were developed, expanded in MFSTEP to three dimensional models coupled to the existing forecasting hydrodynamic models. Parallel to the above, data assimilation techniques for biochemical variables were implemented with a future

aim to achieve full predictive capability.

The ecosystem model developed (BFM) is a continuation of the generic and highly complex model ERSEM which is successfully established in the scientific community. Even though in its preliminary application in the Eastern Mediterranean the model behaviour is distant from being perfect, results are promising for the future. Although not entirely the focus of this paper, simulation results show a good agreement with observations, responding efficiently to the variability in mixing nutrient supply and light conditions, reproducing the full range of scales of variability and of marine ecosystem behaviour from eutrophic in gulfs and shallow coastal waters to extremely oligotrophic in outer areas. Considering that open ocean processes dominate the Eastern Mediterranean ecosystem and that the limited extent of the continental shelf means that the general circulation has a significant influence on coastal processes, some key characteristics as produced by the model are: i) primary production is mainly controlled by mixing processes ii) stratification period is characterised by the development of a deep chlorophyll maximum and a dominant microbial loop iii) in coastal areas the herbivorous food web is more important although the dominant carbon flux along the trophic web can seasonally shift from the herbivorous to the microbial pathway and iv) inputs from rivers and Dardanelles are exported from the coastal to the offshore areas.

Important issues such as the validation of the model with satellite images which have been produced with specific for case I waters, algorithms, the role of viruses and the influence of water inputs particularly in the north Aegean will all be high priority future tasks. Models should provoke questions as well as provide quantitative and qualitative insights (Blackford et al., 2004b), and to this respect the Eastern Mediterranean coupled physical – biological model adequately fulfils its purpose.

The model presented in this work is a significant advancement in the coupled hydrodynamic-ecosystem modelling of Eastern Mediterranean and will form the basis of several modelling studies. It will provide the scientific and technological knowledge to underpin the construction of an operational forecast model for the marine ecosystem and an expert system which can link the model with our knowledge and experi-

ence of the environment. Thus it can make a fundamental contribution to the strategic management of coastal waters where decision support systems are urgently required. Further to the above the EU agreed to an 8% decrease in carbon dioxide emissions from 1990 levels in the period 2008–2012 at the Kyoto conference. Carbon dioxide is

5   the most important of the greenhouse gases, accounting for 80% of the impact. The generic modelling tool developed, can be coupled with atmospheric models to provide a sound scientific and technological basis for the quantification of the role of the Eastern Mediterranean as sources and sinks for carbon dioxide.

Finally with the implementation of data assimilation system for the marine ecosystem
10   of the Eastern Mediterranean will enables us to assess the potential of the modelling system to predict short and long term changes in the marine ecosystem structure. To achieve predictive capabilities, deterministic ecosystem models need to be updated with biological, physical and chemical data at relevant space-time scales. Data assimilation schemes provide the appropriate techniques for updating and initialising models
15   and assessing them in predictive mode. Data assimilation systems for meteorological models and OGCM's are well established in contrast with assimilation in marine ecosystem models which is far less developed. However the growing need for the development of marine operational systems has led to significantly more and more effort being invested in such techniques (Allen et al., 2003; Hoang et al., 1997; Hoteit et al.,
20   2002; Hoteit et al., 2004; Hoteit et al., 2003; Natvik and Evensen, 2003; Triantafyllou et al., 2003a; Triantafyllou et al., 2003b; Triantafyllou et al., 2001). Advanced assimilation filters developed during MFSTEP have been incorporated in the ecosystem model described in this work and are presented in a companion paper in this volume.

References

Aksnes, D. L. and Egge, J. K.: A theoretical model for nutrient uptake in phytoplankton, Mar. Ecol. Prog. Ser., 70, 65–72, 1991.

Alhammoud, B., Beranger, K., Mortier, L., Crepon, M., and Dekeyser, I.: Surface circulation of the Levantine Basin: Comparison of model results with observations, Progress in Oceanography, 66, 299–320, 2005.

Allen, J. I., Ekenes, M., and Evensen, G.: An Ensemble Kalman Filter with a complex marine ecosystem model: Hindcasting phytoplankton in the Cretan Sea, Ann. Geophys., 21, 399–411, 2003.

Allen, J. I., Siddorn, R. J., Blackford, C. J., and Gilbert, J. F.: Turbulence as a control on the microbial loop in a temperate seasonally stratified marine systems model, J. Sea Res., 52, 1–20, 2004.

Azam, F., Fenchel, T., Field, J. G., Gray, J. S., Meyer-Reil, L. A., and Thingstad, F.: The ecological role of water – column microbes in the sea, Mar. Ecol. Prog. Ser., 10, 257–263, 1983.

Azov, Y.: Eastern Mediterranean – a marine desert? EMECS' 90, 23, 225–232, 1991.

Baretta-Bekker, J. G., Baretta, J. W., and Ebenhoh, W.: Microbial dynamics in the marine ecosystem model ERSEM II with decoupled carbon assimilation and nutrient uptake, J. Sea Res., 38, 195–211, 1997.

Baretta-Bekker, J. G., Baretta, J. W., and Rasmussen, E.: The microbial foodweb in the European regional Seas Ecosystem Model, Netherlands Journal of Sea Research, 33, 363–379, 1995.

Baretta, J. W., Ebenhoh, W., and Ruardij, P.: The European Regional Seas Ecosystem Model, a complex marine ecosystem model, Netherlands Journal of Sea Research, 33, 233–246, 1995.

Blackford, C. J., Allen, J. I., and Gilbert, J. F.: Ecosystem dynamics at six contrasting sites: a generic modelling study, J. Mar. Syst., 52, 191–215, 2004a.

Blackford, C. J., Allen, J. I., and Gilbert, J. F.: Ecosystem dynamics at six contrasting sites: a generic modelling study, J. Mar. Syst., 2004b.

Blumberg, A. F. and Mellor, G. L.: A Coastal Ocean Numerical Model. In: J. Sunderman and K. Holtz (Editors), Mathematical Modelling of Estuarine Physics. Proceedings of the International Symposium, Springer-Verlag Berlin, Hamburg, pp. 203–214, 1978.

Blumberg, A. F. and Mellor, G. L.: A description of a three-dimensional coastal ocean circulation

model, in: Three-Dimensional Coastal Ocean Circulation Models, edited by: Heaps, N. S., Coastal Estuarine Science, AGU, Washington, D.C., pp. 1–16, 1987.

Bratbak, G., Heldal, M., Thingsta, T. F., Riemann, B., and Haslnund, O. H.: Incorporation of viruses into the budget of microbial C-transfer. A first approach, Mar. Ecol. Prog. Ser., 83, 273–280, 1992.

Bricaud, A., Bosc, E., and Antoine, D.: Algal biomass and sea surface temperature in the Mediterranean Basin. Intercomparison of data from various satellite sensors, and implications for primary production estimates, Rem. Sens. Environ., 81, 163–178, 2002.

Crise, A., Allen, J. I., Baretta, J., Crispi, G., Mosetti, R., and Solidoro, C.: The Mediterranean pelagic ecosystem response to physical forcing, Prog. Oceanogr., 44, 219–243, 1999.

Droop, M. R.: The nutrient status of algal cells in continuous culture, J. Mar. Biol. Assoc., 54, 825–855, 1974.

Eker-Develi, E., Erkan Kideys, A., and Tugrul, S.: Role of Saharan dust on phytoplankton dynamics in the northeastern Mediterranean, Mar. Ecol. Prog. Ser., 374, 61–75, 2006.

Fuhrman, J. A.: Marine viruses and their biogeochemical and ecological effects, Nature, 399, 541–548, 1999.

Georgopoulos, D., Chronis, G., Zervakis, V., Lykousis, V., Poulos, S., and Iona, A.: Hydrology and circulation in the Southern Cretan Sea during the CINCS experiment (May 1994–September 1995), Prog. Oceanogr., 46, 89–112, 2000.

Gill, A. E.: Atmosphere-Ocean Dynamics, Academic Press, New York, 662pp., 1982.

Heldal, M. and Bratbak, G.: Production and decay of viruses in aquatic environments, Mar. Ecol. Prog. Ser., 72, 205–212, 1991.

Hoang, H. S., De Mey, P., Tallagrand, O., and Baraille, R.: Adaptive filtering: Application to satellite data assimilation in oceanography, J. Dyn. Atmos. Oceans, 27, 257–281, 1997.

Hood, R. R., Laws, A. E., Armstrong, A. R., Bates, R. N., Brown, W. C., Carlson, A. C., Chai, F., Doney, C. S., Falkowski, G. P., Feely, A. R., Friedrichs, A. M. M., Landry, R. M., Moore, J. K., Nelson, M. D., Richardson, L. T., Salihoglu, B., Schartau, M., Toole, A. D., and Wiggert, D. J.: Pelagic functional group modeling: Progress, challenges and prospects, Deep Sea Res. II, 53, 459–512, 2006.

Hoteit, I., Pham, D. T., and Blum, J.: A semi-evolutive partially local filter for data assimilation, Mar. Poll. Bull., 43(7–12), 164–174, 2002.

Hoteit, I., Triantafyllou, G., and Petihakis, G.: Towards a data assimilation system for the Cretan sea ecosystem using a simplified Kalman filter, J. Mar. Syst., 45, 159–171, 2004.

Eastern Mediterranean biogeochemical flux model

G. Petihakis et al.

Title Page

Abstract | Introduction

Conclusions | References

Tables | Figures

|◄ | ►|

◄ | ►

Back | Close

Full Screen / Esc

Printer-friendly Version

Interactive Discussion

Hoteit, I., Triantafyllou, G., Petihakis, G., and Allen, J. I.: A singular evolutive Kalman filter to assimilate real in-situ data in a 1-D marine ecosystem model, Ann. Geophys., 21, 389-397, 2003.

Ignatiades, L., Psarra, S., Zervakis, V., Pagou, K., Souvermezoglou, E., Assimakopoulou, G., and Gotsi-Skreta, O.: Phytoplankton size-based dynamics in the Aegean Sea (Eastern Mediterranean), J. Mar. Syst., 36, 11–28, 2002.

Jaeger, L.: Monatskarten des Niederschlags fur die ganze Erde, Ber. Dtsch. Wetterdienste, 18(1839), 1–38, 1976.

Korres, G. and Lascaratos, A.: A one-way nested eddy resolving model of the Aegean and Levantine basins: Implementation and climatological runs, Ann Geophys., 21, 205–220, 2003.

Krom, M., Groom, S., and Zohary, T.: The Eastern Mediterranean, in: Biogeochemistry of Marine Systems, edited by: Black, K. D. and Shimmield, G. B., Blackwell Publishing, Oxford, 91–126, 2003.

Lykousis, V., Chronis, G., Tselepides, A., Price, N.B., Theocharis, A., Siokou-Frangou, I., Van Wambeke, F., Donavaro, R., Stavrakakis, S., Duineveld, G., Georgopoulos, D., Ignatiades, L., Souvermezoglou, E., and Voutsinou-Taliadourou, F.: Major outputs of the recent multidisciplinary biogeochemical researches undertaken in the Aegean Sea, J. Mar. Syst., 33–34, 313–334, 2002.

McGill, D.: The relative supplies of phosphate, nitrate and silicate in the Mediterranean Sea, Rapports et Proces-Verbaux des Reunions Commission Internationale pour l'Exploration Scientifique de la Mer Mediterranee, 18, 734–744, 1965.

Mellor, G. L.: User's guide for a three-dimensional primitive equation, numerical ocean model (July 1998 version), Princeton University, 1998.

Mihailov, A. A.: On the phytoplankton of the Aegean Sea. Trudy Sevastopol. Biol. St., 17, 3–12, 1964.

Moutin, T. and Raimbault, P.: Primary production, carbon export and nutrients availability in western and eastern Mediterranean Sea in early summer 1996 (MINOS cruise), J. Mar. Syst., 33–34, 273–288, 2002.

Natvik, L. and Evensen, G.: Assimilation of ocean colour data into a biochemical model of the north Atlantic. Part-I. data assimilation experiments, J. Mar. Syst., 40–41, 127–153, 2003.

Parsons, T., Takahashi, M., and Hargrave, B.: Biological oceanographic processes, Pergamon Press, 330pp., 1973.

Pinardi, N. and Masetti, E. L.: Variability of the large scale general circulation of the Mediter-

Title Page

Abstract | Introduction

Conclusions | References

Tables | Figures

|◄ | ►|

◄ | ►

Back | Close

Full Screen / Esc

Printer-friendly Version

Interactive Discussion

ranean Sea from observations and modelling: a review, Palaeogeography, Palaeoclimatology, Palaeoecology, 158, 153–174, 2000.

Proctor, L. M. and Fuhrman, J. A.: Viral mortality of marine bacteria and cyanobacteria, Nature, 343, 60–62, 1990.

5   Sancak, S., Besiktepe, T. S., Yilmaz, A., Lee, M., and Frouin, R.: Evaluation of SeaWifs chlorophyll-a in the Black and Mediterranean Seas, Int. J. Rem. Sens., 26(10), 2045–2060, 2005.

Siokou-Frangou, I., Bianchi, M., Christaki, U., Christou, E. D., Giannakourou, A., Gotsis, O., Ignatiades, L., Pagou, K., Pitta, P., Psarra, S., Souvermezoglou, E., Van Wambeke, F., and
10   Zervakis, V.: Carbon flow in the planktonic food web along a gradient of oligotrophy in the Aegean Sea (Mediterranean Sea), J. Mar. Syst., 33–34, 335–353, 2002.

Suttle, C. A., Chan, A. M., and Cottrell, M. T.: Infection of phytoplankton by viruses and reduction of primary production, Nature, 347, 467–469, 1990.

Theocharis, A., Balopoulos, E., Kioroglou, S., Kontoyiannis, H., and Iona, A.: A synthesis of
15   the circulation and hydrography of the South Aegean Sea and the Straits of the Cretan Arc (March 1994–January 1995), Prog. Oceanogr., 44, 469–509, 1999.

Theocharis, A., Georgopoulos, D., Lascaratos, A., and Nittis, K.: Water masses and circulation in the central region of the Eastern Mediterranean: Eastern Ionian, South Aegean and Northwest Levantine, Deep-Sea Res. II, 40(6), 1121–1142, 1993.

20   Theocharis, A., Klein, B., Nittis, K., and Roether, W.: Evolution and status of the Eastern Mediterranean Transient (1997–1999), J. Mar. Syst., 33–34, 91–116.

Triantafyllou, G., Hoteit, I., and Petihakis, G.: A singular evolutive interpolated Kalman filter for efficient data assimilation in a 3-D complex physical-biogeochemical model of the Cretan Sea, J. Mar. Syst., 40–41, 213–231, 2003a.

25   Triantafyllou, G., Hoteit, I., and Petihakis, G.: The use of global and local EOFs for the assimilation of biochemical data into Cretan Sea ecosystem model, EGS 2003, Geophys. Res. Abstr., 5, 10497, 2003b.

Triantafyllou, G., Hoteit, I., Petihakis, G., Allen, J. I., Pollani, A., and Dounas, C.: Efficient Reduced Kalman Filtering for Assimilating the Spatial and Temporal Variability of the Cre-
30   tan Ecosystem, 33rd international Liege Colloquium on Ocean Dynamics, The use of Data Assimilation in Coupled Hydrodynamic, Ecological and Bio-Geo-Chemical Models of the Ocean, Liege, 2001.

Tselepides, A. and Polychronaki, T.: Pelagic-benthic coupling in the oligotrophic Cretan Sea

Title Page

Abstract   Introduction

Conclusions   References

Tables   Figures

◄◄   ►►

◄   ►

Back   Close

Full Screen / Esc

Printer-friendly Version

Interactive Discussion

(Ne Mediterranean), IMBC, Iraklio, 1996.

Vichi, M., Baretta, J., Baretta-Bekker, J., Ebenhoh, W., Kohlmeier, Ruardij, P., Pinardi, N., and Zavatarelli, M.: European Regional Seas Ecosystem Model III. Review of the biogeochemical equations, www.bo.ingv.it/ersem3/, ERSEM_III_report.lyx,v 1.6 2004/07/28 10:44:29 mav Exp., 2004.

Zohary, T. and Robarts, R. D.: Experimental study of microbial P-limitation in the Eastern Mediterranean, Limnol. Oceanogr., 43, 387–395, 1998.

Eastern Mediterranean biogeochemical flux model

G. Petihakis et al.

Title Page

Abstract	Introduction
Conclusions	References
Tables	Figures

◄ | ►|

◄ | ►

Back | Close

Full Screen / Esc

Printer-friendly Version

Interactive Discussion

EGU

Eastern Mediterranean biogeochemical flux model

G. Petihakis et al.

Table 1. Pelagic state variables. Carbon and Chl units are in mg C/m^3, nutrients are in mmol/m^3.

State variable	Symbol	Constituents
Diatoms (20–200 μm)	P1	C, N, P, Si, Chl
Nanophytoplankton (2–20 μm)	P2	C, N, P, Si, Chl
Picophytoplankton (0.2–2 μm)	P3	C, N, P, Si, Chl
Large phyto (20–200 μm)	P4	C, N, P, Si, Chl
Pelagic bacteria	B1	C, N, P
Heterotrophic nanoflagellates (2–20 μm)	Z6	C, N, P
Microzooplankton (20–200 μm)	Z5	C, N, P
Mesozooplankton (omnivorous)	Z4	C, N, P
Mesozooplankton (carnivorous)	Z3	C, N, P
DOM labile	R1	C
DOM carbohydrates	R2	C, N, P, Si
POC	R6	C, N, P, Si
Nitrate	N3n	N
Ammonium	N4n	N
Phosphate	N1p	P
Silicate	N5s	Si
Reduction equivelants	N6r	S
Oxygen	O2o	O$_2$

EGU

Table 2. Food matrix.

Preys/Predators	Z6	Z5	Z4	Z3
P1	0.0	0.0	1.0	0.0
P2	0.2	1.0	0.4	0.0
P3	1.0	0.1	0.0	0.0
P4	0.0	0.0	1.0	0.0
B1	1.0	0.1	0.0	0.0
Z6	0.2	1.0	0.0	0.0
Z5		1.0	1.0	0.0
Z4			1.0	1.0
Z3				1.0

EGU

Eastern Mediterranean biogeochemical flux model

G. Petihakis et al.

Table 3. Optical parameters.

Parameter	Symbol	Value
Background extinction coefficient (m^{-1})	p_eps0	0.04
Extinction coefficient of silt ($m^{-1}\,mg^{-1}$)	p_epsESS	$0.04e^{-3}$
Extinction coefficient of phyto ($m^{-1}\,mgC^{-1}$)	p_epsChla	$10.0e^{-3}$
Extinction coefficient of POC ($m^{-1}\,mgC^{-1}$)	p_epsR6	$0.1e^{-3}$
Proportion of irradiance photosynthetically available	p_PAR	0.5
Adaptation depth (m)	paddepth	10

EGU

Table 4. Parameters for the primary producers.

Parameter	Symbol	P1	P2	P3	P4
Characteristic Q10	p_q10	2.0	2.0	2.0	2.0
Max. productivity at 10°C (day^{-1})	p_sum	2.5	3.0	3.5	1.5
Rest respiration at 10°C (day^{-1})	p_srs	0.1	0.05	0.1	0.1
Activity respiration (fraction of production)	p_pu_ra	0.1	0.1	0.2	0.1
Activity excretion (fraction of production)	p_pu_ea	0.05	0.1	0.1	0.15
Redfield N/C ratio (mmol N/mgC)	p_qnRc	0.0126	0.0126	0.0126	0.0126
Redfield P/C ratio (mmol P/mgC)	p_qpRc	0.786e-3	0.786e-3	0.786e-3	0.786e-3
Redfield Si/C ratio (mmol Si/mgC)	p_qsRc	0.01	0.0	0.0	0.0
Mult. Factor Max. N/C ratio	p_xqn	2.0	2.0	2.0	2.0
Mult. Factor Max. P/C ratio	p_xqp	2.0	2.0	2.0	2.0
Min. N/C ratio (mmol N/mgC)	p_qnlc	0.00687	0.00687	0.00687	0.00687
Min. P/C ratio (mmol P/mgC)	p_qplc	0.4288e-3	0.4288e-3	0.4288e-3	0.4288e-3
Min. Si/C ratio (mmol Si/mgC)	p_qslc	0.007	0.0	0.0	0.0
Uptake parameter for N (m^3/mgC day)	p_qun	0.0025	0.0025	0.0025	0.0025
Uptake parameter for PO$_4$ (m^3/mgC day)	p_qup	0.0025	0.0025	0.0025	0.0025
Uptake parameter for SiO$_4$ (m^3/mgC day)	p_qus	0.0025	0.0	0.0	0.0
Nutrient stress sinking threshold	p_esNI	0.70	0.75	0.75	0.75
Background sinking rate (m/day)	p_rPim	0.25	0.0	0.0	0.25
Nutrient stress sinking (m/day)	p_res	5.0	0.0	0.0	3.0
Half value of SiO$_4$ limitation (mmol Si/m^3)	p_chPs	1.0	0.0	0.0	0.0
Half value of NO$_3$ uptake (mmol N/m^3)	p_lN4	1.0	0.5	0.1	1.0
Max chl to carbon ratio (mgChl/mgC)	p_qchlc	0.05	0.03	0.07	0.02
Slope of $P-I$ curve (W m^{-2})$^{-1}$ d^{-1}	p_alpha_chl	1.38e^{-5}	1.52e^{-5}	1.52e^{-5}	1.38e^{-5}
Chlorophyll destruction factor	p_sdchl	0.2	0.2	0.2	0.2

Table 5. Parameters for the decomposers and the detritus.

Parameter	Symbol	B1
Characteristic Q10	p_q10	2.95
Half saturation of O_2 (mmol/ m^3)	p_chdo	30.0
Max. productivity at 10°C (day^{-1})	p_sum	8.38
Rest respiration at 10°C (day^{-1})	p_srs	0.01
Decrease in assimilation efficiency at low O_2 conc.	p_puo	0.2
Assimilation efficiency	p_pu	0.4
Mortality factor	P_sd	0.0
Redfield N/C ratio (mmol N/mgC)	p_qnc	0.017
Redfield P/C ratio (mmol P/mgC)	p_qpc	0.0019
Min. N/C ratio (mmol N/mgC)	p_qlnc	0.0085
Min. P/C ratio (mmol P/mgC)	p_qlpc	0.95 e-3
Uptake parameter for NO_3 and NH_4 (m^3/mgC day)	p_qun	0.05
Uptake parameter for PO_4 (m^3/mgC day)	p_qup	0.005
Half value of NO_3 uptake	p_lN4	0.05
Preference for DOC (day^{-1})	p_suR1	0.5
Preference for DOC (sugars) (day^{-1})	p_suR2	0.025
Preference for POC (day^{-1})	p_suR6	0.1
Detritus sinking rate (m/day)	p_rR6m	3.0
Relative nitrification rate (day^{-1})	p_sN4N3	0.01
Relative nitrification rate at 10°C	p_q10N4N3	2.367
Relative denitrification rate (day^{-1})	p_sN3O4n	0.35
Relative reoxidation rate of reduction equivalents (day^{-1})	p_rOS	0.05
Relative regeneration rate of dissolved silica (day^{-1})	p_sR6N5	0.1
Relative regeneration rate of dissolved silica at 10°C	p_q10R6N5	1.49
Oxygen half saturation regulating factor (mmol/ m^3)	p_clO2o	10.0

Title Page

Abstract | Introduction

Conclusions | References

Tables | Figures

◄ | ►

◄ | ►

Back | Close

Full Screen / Esc

Printer-friendly Version

Interactive Discussion

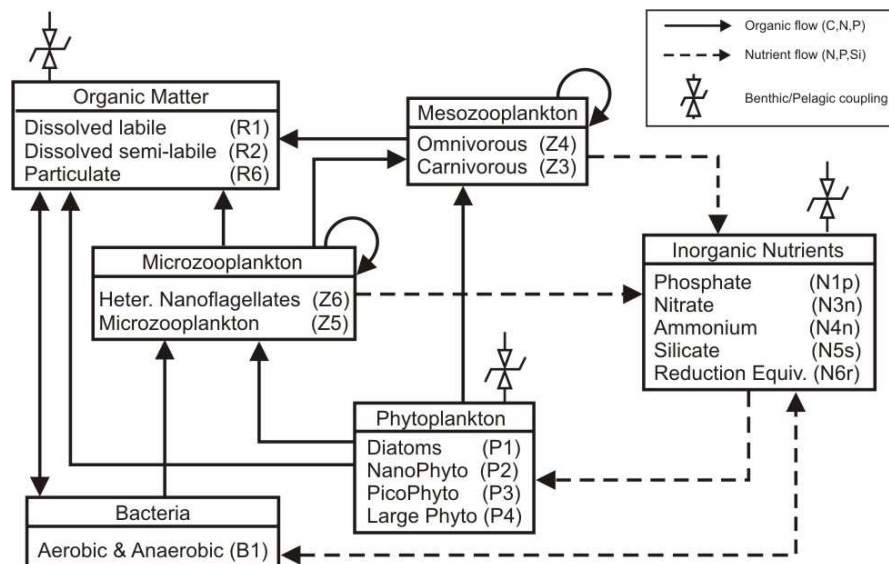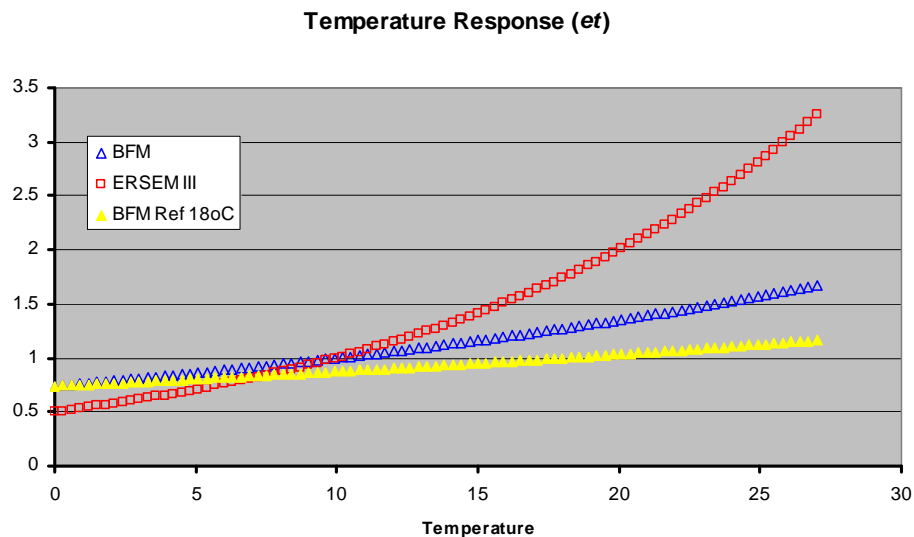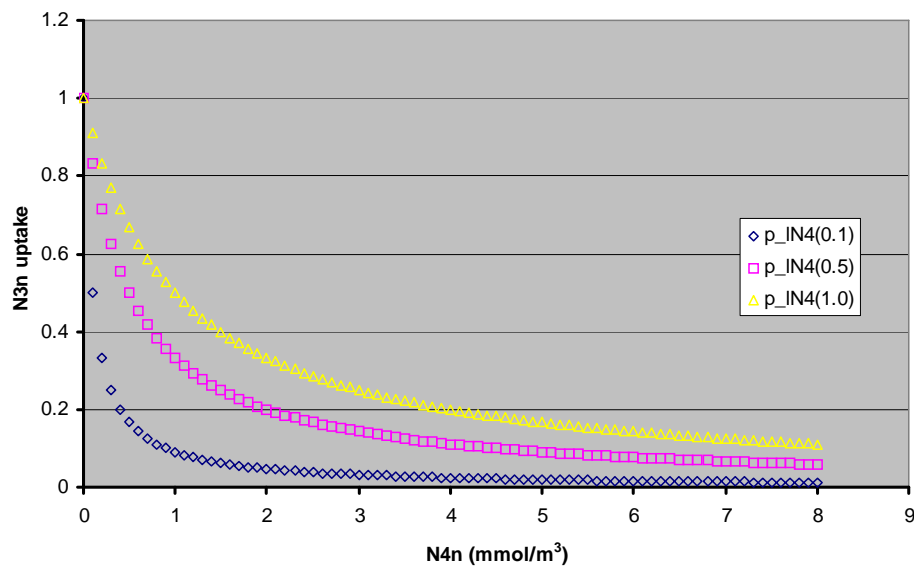**Eastern Mediterranean biogeochemical flux model**

G. Petihakis et al.

**Table 6.** Parameters for the consumers.

Parameter	Symbol	Z6	Z5	Z4	Z3
Characteristic Q10	p_q10	2.0	2.0	2.0	2.0
Half saturation of O_2 (mmol/ m^3)	p_chro	7.8	7.8	–	–
Max. productivity at 10°C (day^{-1})	p_sum	5.0	2.0	0.5	0.3
Rest respiration at 10°C (day^{-1})	p_srs	0.02	0.02	0.02	0.01
Assimilation efficiency in microzoo	p_pu	0.3	0.5	–	–
Assimilation efficiency in mesozoo	p_pul_u	–	–	0.6	0.6
Activity excretion (fraction of production)	p_pu_ea	0.5	0.5	–	–
Fraction of excretion passed to DOM	p_pe_R1	0.7	0.7	–	–
Excretion to POC (fraction of food eaten)	p_pel_R6	–	–	0.35	0.3
Oxygen dependent mortality (day^{-1})	p_sdo	0.05	0.05	0.4 e-3	0.4 e-3
Natural mortality (day^{-1})	p_sd	–	–	0.01	0.01
Density dependent mortality (day^{-1})	p_sds	–	–	2.0	2.0
Max. N/C ratio in microzoo (mmol N/mgC)	p_qn_mz	0.0167	0.0167	–	–
Max. P/C ratio in microzoo (mmol P/mgC)	p_qp_mz	0.185 e-3	0.185 e-3	–	–
N/C ratio in mesozoo (mmol N/mgC)	p_qnc	–	–	0.015	0.015
P/C ratio in mesozoo (mmol P/mgC)	p_qpc	–	–	0.167 e-2	0.167 e-2
Damping coefficient of excretion (day^{-1})	p_stemp	0.5	0.5	–	–
Half saturation food uptake (mgC/ m^3)	p_chuc	50.0	50.0	–	–
Lower threshold for feeding (mgC/ m^3)	p_minfood	30.0	30.0	–	–
Search volume (m^3)	p_vum	0.016	0.032	–	–

Table 7. Biological parameters measured in the North, South Aegean and west of Dardanelles during March and September (Ignatiades et al., 2002; Siokou-Frangou et al., 2002).

	N. Aegean		S. Aegean		Dardanelles	
	March-97	Sept-97	March-97	Sept-97	March-97	Sept-97
Chl-a (mgC/m$^{3)}$)	0.379±0.262	0.260±0.126	0.301±0.105	0.119±0.091		
Picophyto (mgC/m^2)	1320±384 (81%)	817±196 (76%)	856±311 (57%)	465±64 (72%)	2052 (80%)	1326±539 (82%)
Bacteria (mgC/m^2)	1406±327	1470±273 (69%)	1423±43 (75%)	1505±432 (59%)	1403±142	1251±107 (66%)
Heter. Nanoflagellates (mgC/m^2)		418±90 (20%)	192±54 (10%)	812±376 (32%)		301±31 (16%)
Primary Prod. (mgC/m^{2}d)	1406±362	253±70	574±176	218 + 63	2339±905	221±13
Bacteria Prod. (mgC/m^{2}d)	48±31	60±11	75±9	58±13	110±77	71

Fig. 1. Food web.

Eastern Mediterranean biogeochemical flux model

G. Petihakis et al.

Fig. 2. Temperature response in BFM with standard reference temperature (10˚C) and Eastern Mediterranean reference temperature (18˚C) and ERSEM III (10˚C).

Fig. 3. Uptake preference for nitrate.

EGU
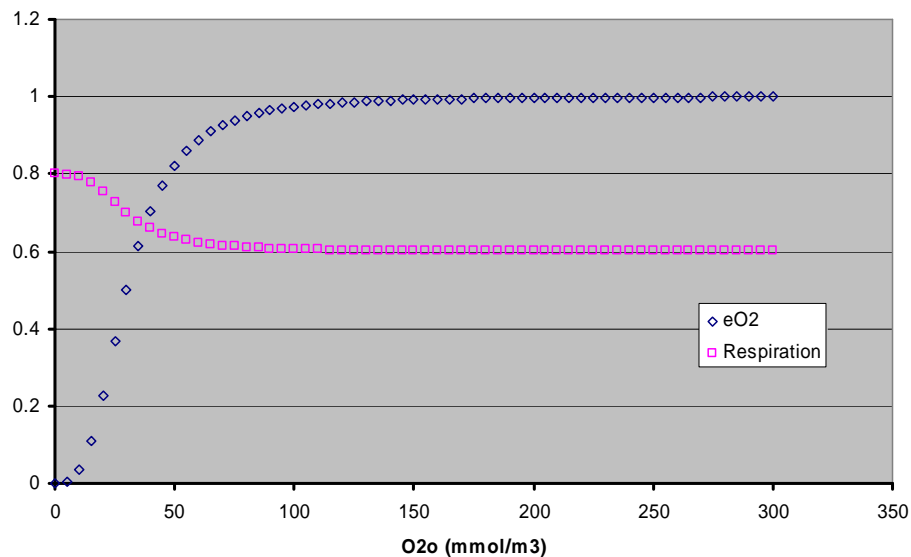
Fig. 4. Oxygen factor (eO2) and activity respiration rate.

Eastern Mediterranean biogeochemical flux model

G. Petihakis et al.
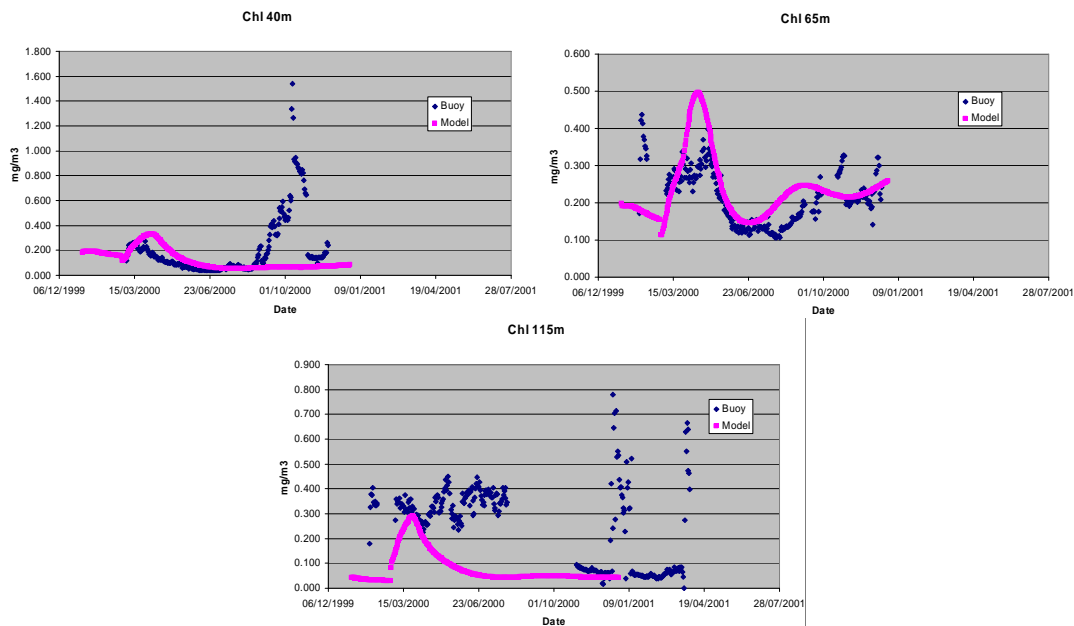
Fig. 5. Comparison of 1-D model Chl-a concentration at various depths against M3A buoy data.

EGU
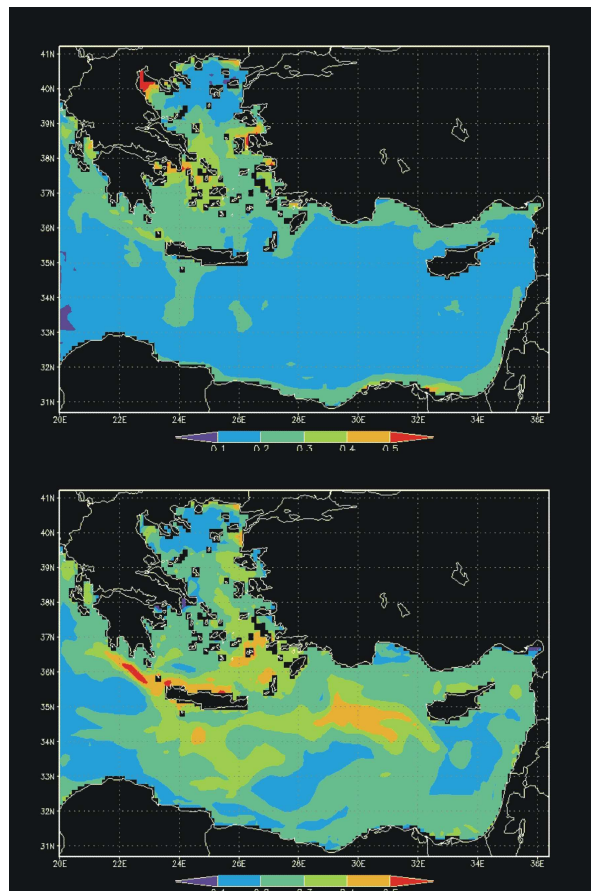
Fig. 6. Mean Chl-a concentrations (mg/m^3) in March (top) and September (bottom).
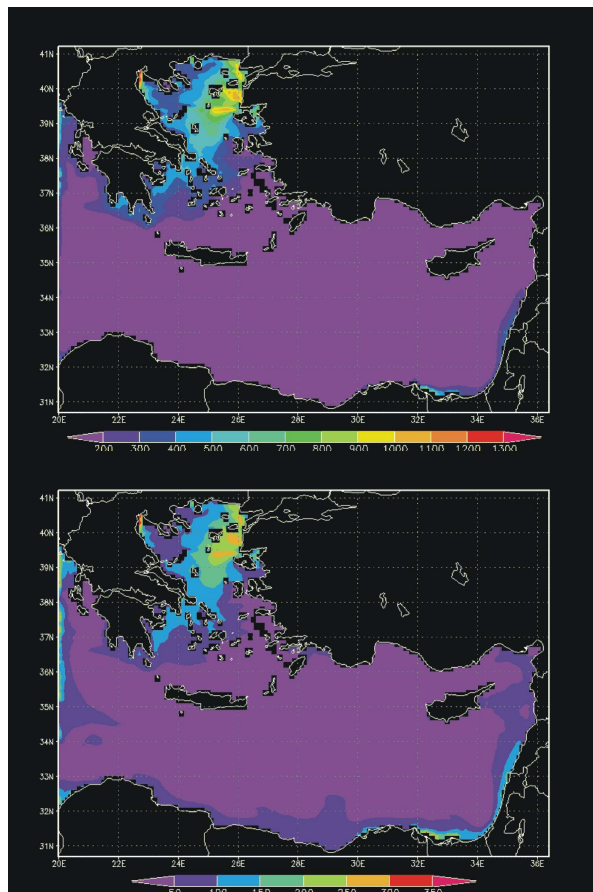
Fig. 7. Integrated primary productivity (mgC/m^{2}d) in March (top) and September (bottom)
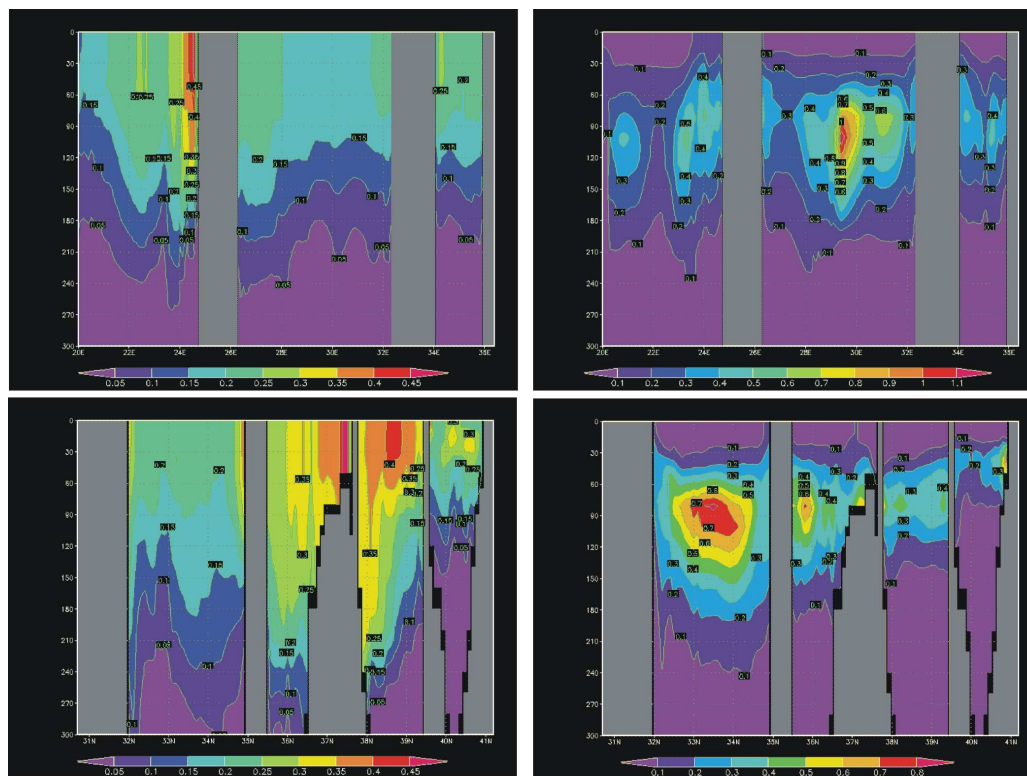
Fig. 8. Vertical cross sections of Chl-a concentrations (mg/m^3) across latitude 35° N (top row), and longitude 25° E (bottom row) in March (left column) and September (right column).

EGU
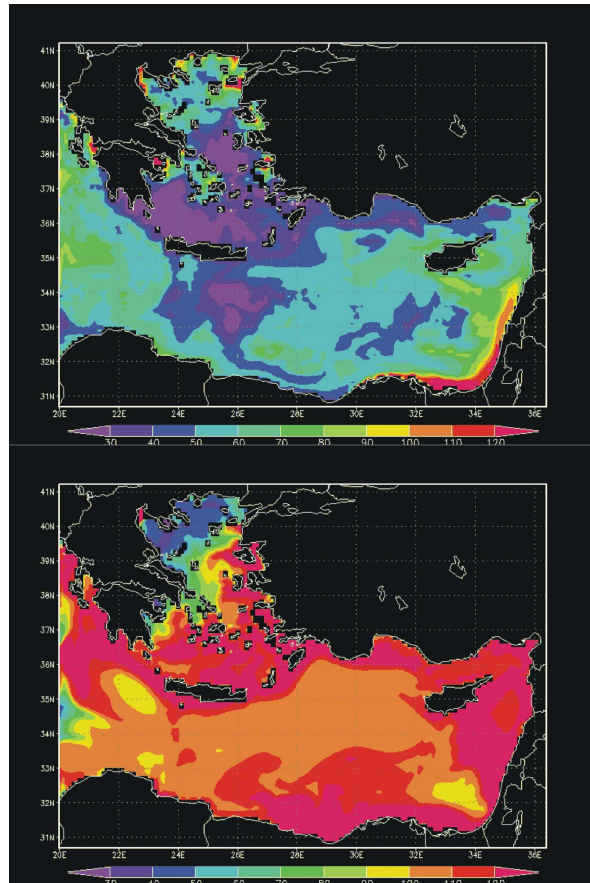
Fig. 9. Integrated bacterial productivity (mgC/m^{2}d) in March (top) and September (bottom).
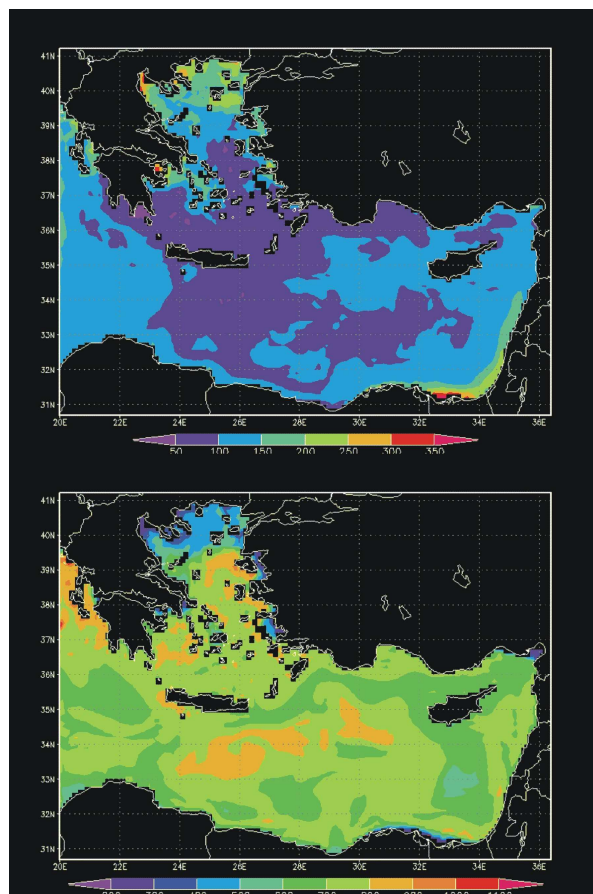
Fig. 10. Integrated heterotrophic flagellate biomass (mgC/m^2) in March (top) and September (bottom),